Meteorological conditions of the stratosphere for the CRISTA 2 campaign, August 1997

G. Günther and D. S. McKenna[1]
Institute for Stratospheric Chemistry (ICG-1), Research Center Jülich, Jülich, Germany

R. Spang[2]
Department of Physics, University of Wuppertal, Wuppertal, Germany

Received 29 March 2001; revised 28 June 2001; accepted 29 June 2001; published 29 October 2002.

[1] During the CRISTA 2 campaign in August 1997 the Antarctic polar vortex according to UK Met Office (UKMO) data was strong but temporarily disturbed by planetary waves. This winter was in general warmer than the five previous winters; nevertheless, temperatures cold enough to allow the formation of nitric acid trihydrate (NAT) and ice particles occurred throughout the period from mid-June to the end of August. The cold vortex core developed in the potential temperature range from 400 to 700 K at the beginning of the winter, initially centered at 600 K but slowly progressing downward to 450 K in the subsequent months. The vortex disturbances showed a clear zonal wave number 1 and 2 pattern. This planetary wave activity caused a strong day-to-day fluctuation of the vortex shape. During August when the second Cryogenic Infrared Spectrometers and Telescopes for the Atmosphere (CRISTA 2) mission took place the vortex was elongated toward the southern Atlantic Ocean, processing slowly eastward. The perturbation of the vortex was associated with air masses transported from middle and low latitudes into the polar region in small-scale streamers. Similarly, tongues of vortex air peeled off the vortex edge and moved equatorward, enhancing the exchange between polar regions and the tropics. In addition, the disturbance of the vortex led to the generation of filaments at the inner side of the vortex edge, thus covering the vortex interior with small-scale structures. A comparison between CRISTA observations and potential vorticity derived from UKMO data shows discrepancies concerning small-scale structures. High-resolution potential vorticity fields calculated from reverse domain filling trajectory simulations on isentropic surfaces based on horizontal winds from UKMO analyses and vertical motion from diabatic calculations are much more consistent with the measurements. Both observation and reverse domain filling (RDF) simulations show the strong atmospheric variability of this period of unusual enhanced planetary wave activity in the Southern Hemisphere. *INDEX TERMS:* 3332 Meteorology and Atmospheric Dynamics: Mesospheric dynamics; 3334 Meteorology and Atmospheric Dynamics: Middle atmosphere dynamics (0341, 0342); 0341 Atmospheric Composition and Structure: Middle atmosphere—constituent transport and chemistry (3334); *KEYWORDS:* CRISTA 2, satellite observations, Antarctic stratosphere, stratospheric meteorology, atmospheric transport, planetary waves

Citation: Günther, G., D. S. McKenna, and R. Spang, Meteorological conditions of the stratosphere for the CRISTA 2 campaign, August 1997, *J. Geophys. Res.*, *107*(D23), 8084, doi:10.1029/2001JD000692, 2002.

1. Introduction

[2] The Cryogenic Spectrometers and Telescopes for the Atmosphere experiment (CRISTA) is a limb-scanning instrument, which measures the thermal emission (4–71 μm) of 18 trace gases and aerosols. The instrument was flown in space twice (by means of the NASA Space Shuttle) for a measurement period of around one week in November 1994 (5–12) and August 1997 (8–16). CRISTA is specially designed for high spatial resolution in all three dimensions by using three telescopes looking 18° apart [*Offermann et al.*, 1999]. Through this approach, a horizontal resolution of around 200 km along and 600 km across the satellite orbit track was achieved. During the second mission the meridional coverage from 74°S–74°N allowed extensive probing of the south polar vortex for mid-winter conditions. Several photochemical active trace gases like O_3, $ClONO_2$, HNO_3, NO_2, N_2O_5 as well as the inert tracers CFC11, N_2O,

[1]Now at National Center for Atmospheric Research, Boulder, Colorado, USA.
[2]Now at EOS Space Research Center, University of Leicester, UK.

0148-0227/02/2001JD000692

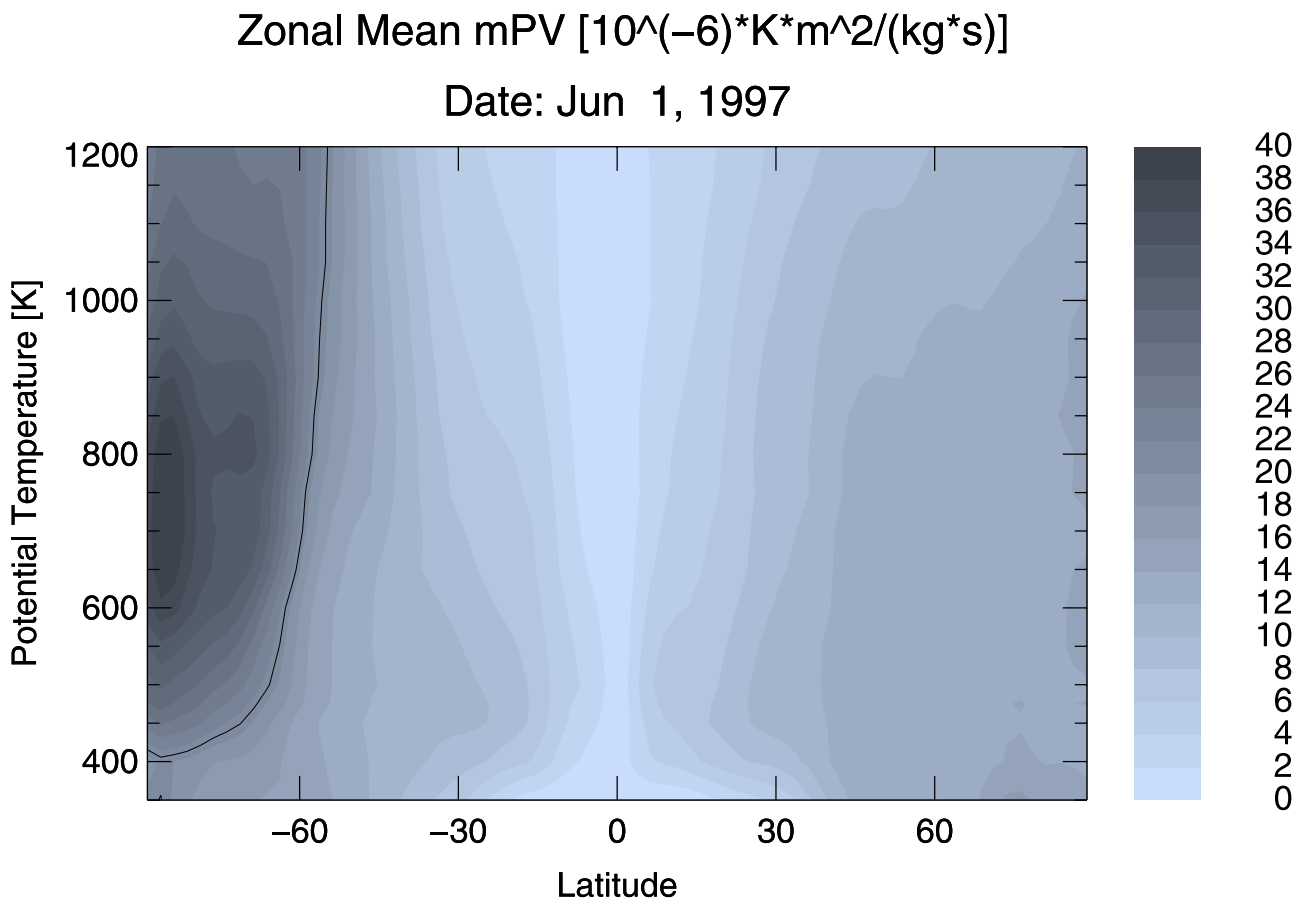

Figure 1. Absolute value of the zonal mean modified PV on 1 June 1997. The thick black line (21 PVU) indicates the vortex edge region.

and CH_4 have been measured in the entire stratosphere with a vertical resolution of around 2 km [*Grossmann et al.*, 2002]. High-reaching tropical clouds around the tropopause and polar stratospheric clouds (PSCs) in the Antarctic lower stratosphere have also been frequently observed. The campaign has comprised several validation measurements, rocket and balloon launches (temperature and ozone), like airplane flights (tropospheric water vapor), and large number of parallel operating ground based instruments all over the world [*Lehmacher and Offermann*, 1997]. This paper describes the meteorological conditions of the stratosphere before and during the second CRISTA campaign. All meteorological data used are taken from the UK Met Office (UKMO) stratosphere-troposphere assimilation system [*Swinbank and O'Neill*, 1994]. Potential temperature (Θ) and potential vorticity (PV) are derived from the data sets to illustrate the dynamical behavior of the Antarctic stratosphere. PV is commonly used to describe the location and the temporal evolution of the polar vortex throughout the winter. Strong horizontal PV gradients on isentropic levels (i.e., surfaces of constant potential temperature Θ) denote the edge of the polar vortex, representing a barrier to quasi-horizontal transport in the winter stratosphere.

[3] Because of its exponential increase with height it is difficult to compare horizontal PV maps at different potential temperature levels or to view horizontal variations in a vertical cross section of the atmosphere. Therefore the so-called modified potential vorticity (mPV) is calculated additionally from the data sets. This is done by scaling PV with the factor $(\Theta/\Theta_0)^{\frac{9}{2}}$ with Θ_0 being a reference level (420 K), thus removing much of the density dependency of PV. The scale factor maintains the structure of PV on any given isentropic surface and preserves the important conservation properties of PV [*Lait*, 1994]. This gives a similar range of values for mPV on isentropic surfaces throughout the stratosphere.

[4] Figure 1 shows the absolute value of the zonal mean mPV for the beginning of June for a height range from 350 to 1200 K. The incipient Antarctic winter vortex was centered near the 750 K isentropic level in early winter. The vortex already extended from 600 K up into the upper stratosphere with the vortex edge being near 70°S. The 21 PVU contour line shown by the thick black line in Figure 1 is centered in the region of strong horizontal mPV gradients and will be used to roughly indicate the vortex edge region. The potential vorticity in the northern summer hemisphere was devoid of significant features. The winds in boreal summer stratosphere were mainly weak easterlies, most of the vorticity seen was planetary.

[5] Although the mPV distribution gives the impression that the Antarctic vortex is strongest in the middle stratosphere it should be noted that this is an artifact of the vertical scaling. The scaling conserves the horizontal but not

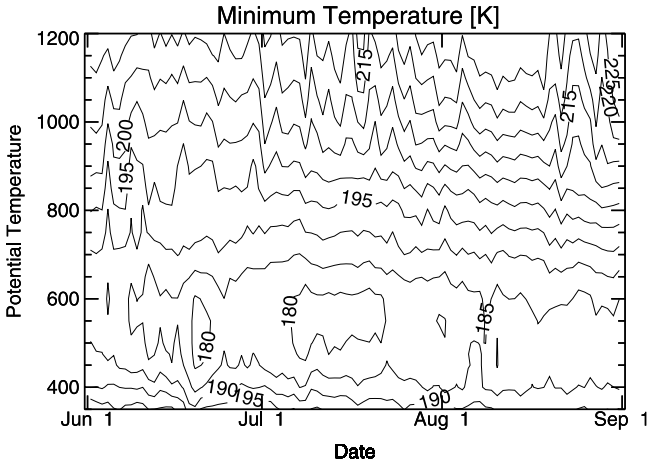

Figure 2. Minimum temperatures for the Antarctic stratosphere from June to August 1997 between 350 and 1200 K.

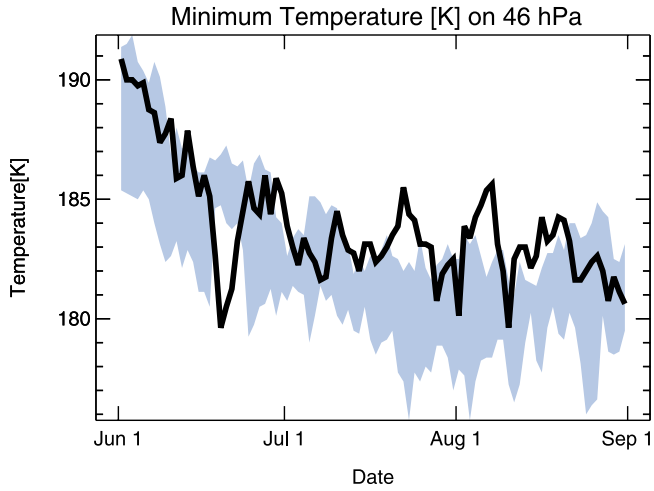

Figure 3. Temporal evolution of the minimum temperature on the 46 hPa pressure level in Kelvin. The shaded area shows the range of minimum temperatures of the five Antarctic winters 1992 to 1996.

the vertical structure of the PV. Thus the absolute values of mPV on different potential temperature levels should not be compared.

2. Analysis

[6] The austral winter of 1997 started with minimum temperatures below 190 K in the lower stratosphere around the 600 K level. As noted, the formation of the polar vortex centered at 750 K had begun at that time (see Figure 1). Over time the vortex air cooled down to values below 180 K between the end of June and August. Having developed at 600 K this cold core descended gradually to 450 K in August (see Figure 2).

[7] Figure 3 shows the temporal evolution of the minimum temperature on the 46 hPa pressure level (approximately 500 K) from June to August. The shaded area represents the range of minimum temperatures of the Antarctic winters from 1992 to 1996. Apart from a short period of cold temperatures in the second half of June, the Antarctic winter of 1997 appears to be in general warmer than the other winters. Especially during an extended period at the end of July and most of August the minimum temperatures are significantly higher than in the five preceding winters. Although the lower stratosphere was warmer in this winter than usual, temperatures were still well below 190 K, thus allowing the formation of PSCs which consist of NAT and ice particles. The exact temperatures for the existence of PSCs depend on altitude, HNO_3 and H_2O partial pressures [see, e.g., *Peter*, 1997].

[8] The decrease of temperatures in the Antarctic lower stratosphere and the resulting increase of the mean meridional temperature gradients through the constraints imposed by thermal wind balance led to a strengthening of the polar night jet. The evolution and strength of the vortex can be tracked through the area weighted mean value of the mPV inside the vortex as shown in Figure 4. The vortex increased strongly in the middle stratosphere between 550 and 1000 K from June until the end of July. In the beginning of August shortly before the CRISTA 2 mission took place this evolution was slowed down and, in some height regions, even inverted. A decrease in strength of the vortex can be observed especially between 550 and 700 K, followed by a similar feature between 800 and 1000 K in the second half of August.

[9] The weakening of the Antarctic vortex during August in both the lower and the middle stratosphere was caused by strong disturbances initiated by planetary waves forcing the stratosphere from below, leading to an enhanced exchange of air masses between lower latitudes and the polar regions, thus consequently increasing mean temperatures in the polar lower stratosphere and initiating large-scale mixing in the surf zone and small-scale mixing at the vortex edge. While strong planetary waves propagating upward through the stratosphere in winter are very common in the Northern Hemisphere, where they cause enhanced variability, they are not very often observed in the Southern Hemisphere with that intensity. Because of less perturbation the Antarctic vortex usually is much colder and remains a closed entity

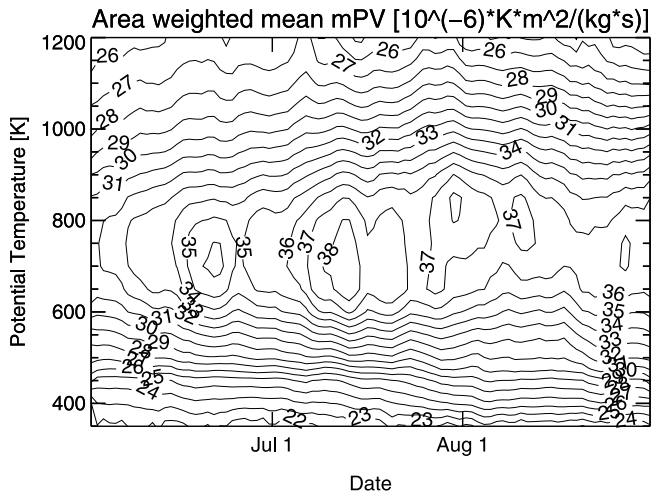

Figure 4. Area weighted mean value of modified PV inside the Antarctic vortex (indicated by the −21 PVU contour line) from June to August 1997 between 350 and 1200 K.

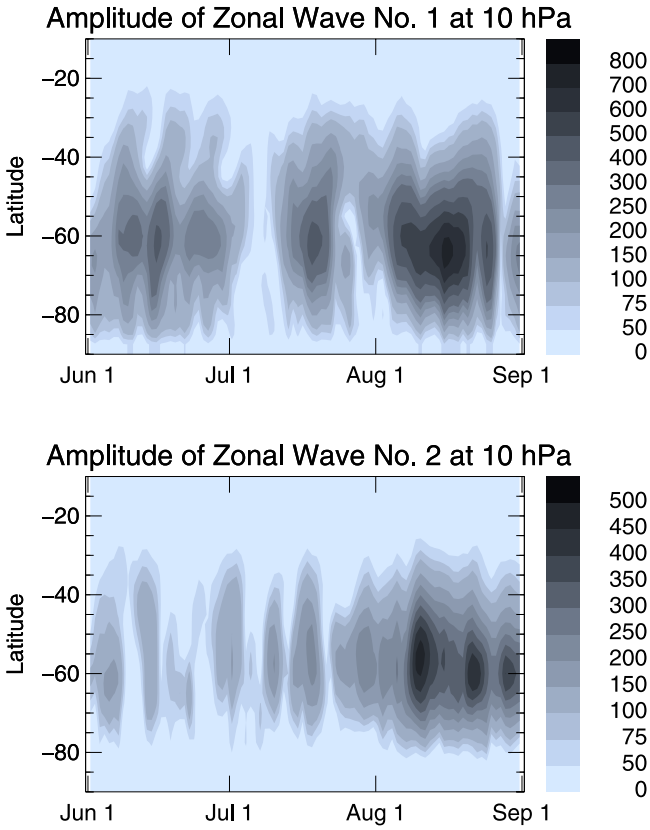

Figure 5. Amplitude of zonal wave 1 (upper panel) and 2 (lower panel) in the Southern Hemisphere as a function of time and latitude for the 10 hPa pressure level (in meters).

for a longer time than the Arctic vortex [see, e.g., *Andrews et al.*, 1987].

[10] In order to investigate the wave characteristics of the considered winter episode a spectral analyses of the geopotential height field was carried out. To show the spatial structure of the main wave components in the Southern Hemisphere during the Antarctic winter horizontal and vertical cross sections of the amplitude of zonal wave 1 and 2 as a function of time will be presented. Figure 5 shows the amplitudes of zonal wave 1 and 2 in the Southern Hemisphere as a function of time and latitude on the 10 hPa pressure level. The main wave activity of both zonal wave 1 and 2 is centered at 60°S with amplitudes falling to low values poleward of 80°S and equatorward of 40°S. The largest amplitudes occur during August with values of 750 m and 475 m for the zonal wave 1 and 2, respectively, coinciding with the strongest perturbation of the Antarctic vortex (see Figure 4).

[11] The vertical structure of the zonal waves 1 and 2 is shown in Figure 6. The first zonal wave 1 event in June is strongest in the middle stratosphere and the wave is strongly damped in the upper stratosphere. No significant zonal wave 2 activity can be observed during this time. The zonal wave 1 events later in the year, especially during August, can be observed throughout the whole stratosphere and lower mesosphere and are accompanied by enhanced zonal wave 2 activity. Apparently for all episodes with large amplitudes the growth of zonal wave 1 and 2 occur in the troposphere as well as in the stratosphere, indicating that the waves are forced in the troposphere and propagate upward into the stratosphere.

[12] A similar analysis carried out for the winters from 1992 to 1996 (not shown here) reveals that the wave activity during the considered episode was stronger and continued for a longer time than in any of the corresponding episodes of the preceding five Antarctic winters. In an analysis of ten years of NMC data from 1979 to 1988, *Manney et al.* [1991] showed that the amplitudes in geopotential height of zonal wave 1 and 2 at 10 hPa in the Southern Hemisphere were in general below 600 m and 400 m, respectively. Only three of the investigated winters showed amplitudes comparable or higher for zonal wave 1 than in 1997, whereas in only four winters values significantly higher for zonal wave 2 were observed. In the most disturbed years 1986 and 1988 the peak values reached 1400 m and 800 m in late winter or early spring. The results of this analysis and the one carried out by *Manney et al.* [1991] and *Riese et al.* [2001] suggest, that the wave activity due to zonal wave 1 and 2 during the Antarctic winter 1997 was stronger than in most other years considered.

[13] The effects of the enhanced planetary wave activity on the dynamics of the stratosphere of the Southern Hemisphere in general and on the evolution of the Antarctic polar vortex in particular can be studied best by examining the horizontal distributions of mPV and temperature. The interaction of the two major wave components led to a strong distortion of the polar vortex in the middle stratosphere. The vortex was forced into a long stretched elliptical shape

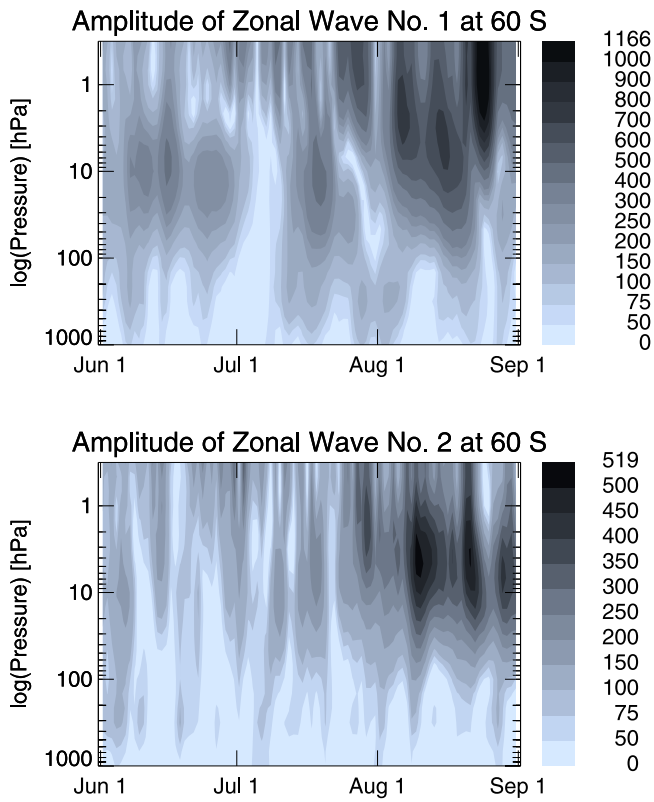

Figure 6. Amplitudes of zonal wave number 1 (upper panel) and (lower panel) 2 of the geopotential height field (in meters) at 60°S for the episode June to August 1997.

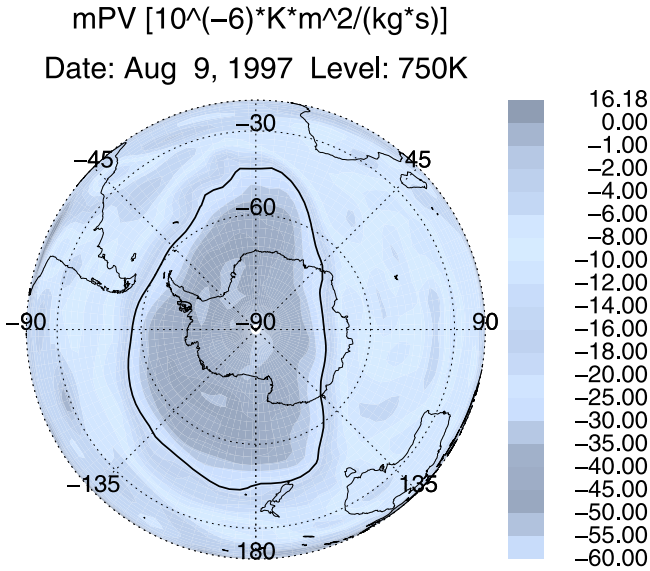

Figure 7. Modified PV on the 750 K isentropic surface on 9 August 1997. The thick black line denotes the vortex edge. See color version of this figure at back of this issue.

slowly rotating eastward about the South Pole during the CRISTA 2 mission from 7 August to 16 August.

[14] On 9 August the ozone poor vortex air moved over New Zealand in the middle stratosphere (Figure 7), while in the lower stratosphere air with low ozone values originating in the subtropics was transported into this region (not shown). The juxtaposition of these two events lead to record low ozone column densities over New Zealand [*Brinksma et al.*, 1998].

[15] The horizontal temperature distribution in the lower stratosphere (Figure 8, left panel) also shows the distinct wave pattern consisting of a strong zonal wave 1 being superimposed by a zonal wave 2, both being in phase with each other. Although the vortex was disturbed, the low-temperature area remained still within the boundaries of the vortex. However, small parts of the vortex near the vortex edge appear to have been much warmer with temperatures around 200 K. Another interesting feature is the cold region having developed near the vortex edge at 160°W. The low temperatures in this area were due to a tropospheric anti-cyclonic high-pressure system leading to an uplift of the tropopause (Figure 9) and subsequent adiabatic cooling of air masses. This meteorological situation often leads to a so-called ozone minihole *McKenna et al.* [1989]. As a consequence of the higher tropopause, a larger proportion of the total ozone column is made up of relatively ozone-poor tropospheric air, leading to values of total ozone being correspondingly lower in this region. The reduction in total ozone is indicated by measurements of both CRISTA 2 and the GOME instrument on board the ERS-2 satellite [*Hild et al.*, 1999]. Although the minihole does not directly contribute to the ozone decline, there may be an influence on the ozone distribution through the dynamically induced cool-

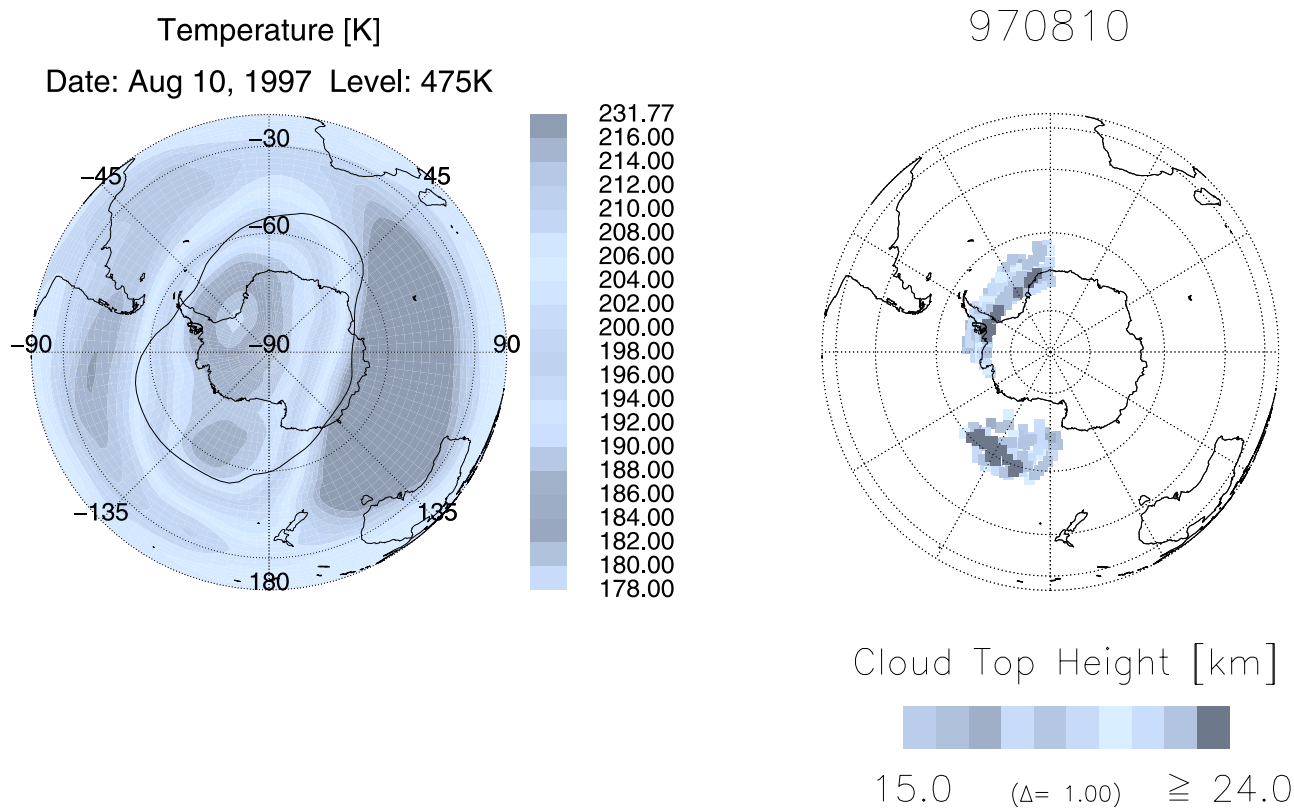

Figure 8. Temperature distribution on the 475 K isentropic level (left) and cloud top height calculated from CO_2 and aerosol measurements by CRISTA 2 (right) for 10 August. The thick black line in the left panel denotes the vortex edge. See color version of this figure at back of this issue.

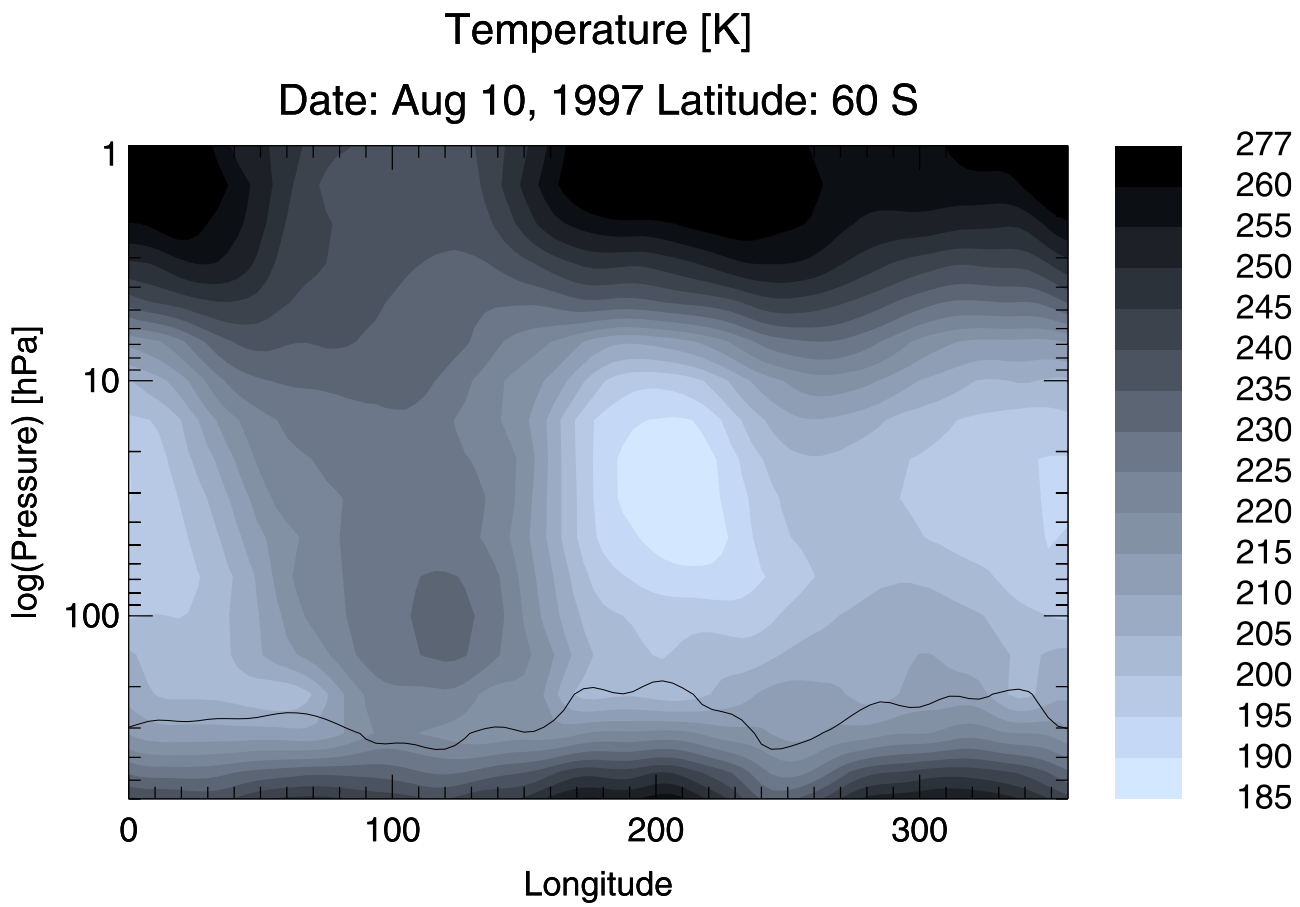

Figure 9. Temperature distribution for 10 August along the 60°S latitudinal circle. The thick black line denotes the position of the dynamical tropopause identified by the −3.5 PVU [*Hoerling et al.*, 1991].

ing. The temperature in both cold areas were low enough to allow the existence of polar stratospheric clouds. As indicated by the position of the vortex edge there is a substantial flow through the regions of cold temperatures, leading to a large volume of air being processed here. Figure 8 (right panel) shows the cloud top heights calculated from CO_2 and aerosol radiance measurements made by the CRISTA instrument on 10 August [*Spang et al.*, 2001]. These results suggest that polar stratospheric clouds formed in both of the cold areas in height regions between 15 and 24 kilometers. The existence of polar stratospheric clouds in these areas are supported by the HNO_3 measurements of CRISTA, indicating denitrification inside the vortex.

[16] On 12 August the vortex had continued its eastward rotation about the South Pole (Figure 10, upper left panel). Two tongues of air masses with low absolute mPV values from middle and low latitudes were transported poleward along the vortex edge thus increasing the mPV gradient across the vortex border. The more pronounced tongue was made up by air masses moving poleward from the South Pacific over South America, and back equatorward on its way toward southern Africa. A less distinctive tongue of air masses was moving from the Indian Ocean toward Antarctica. Being forced to move across the latitudinal circles, the air masses began to spin up anticyclonically conserving PV (and mPV). The formation of a big anticyclonic structure over the South Atlantic with embedded air masses showing low mPV values could be observed. The flow associated with the anticyclone located near New Zealand started to draw material from the Antarctic vortex forming a tongue like structure, thus eroding the vortex edge. To the west of this feature another less pronounced tongue of air originating in the vortex edge could be observed.

[17] For a better comparability between UKMO data and CRISTA measurements the locations of the measurements taken asynoptically during a certain interval of time are mapped forward to a synoptic time using the trajectory model described by *McKenna et al.* [2002]. This is done under the assumption that the lifetimes of the atmospheric constituents shown are long compared to the time interval used, thus considering these constituents as inert tracers.

[18] A comparison between the mPV distribution shown in Figure 10 (upper left panel) and ozone measurements taken by CRISTA and mapped to 12 August (Figure 10, lower left panel) shows in general good agreement between these data and the mPV calculated from UKMO data, although there are some discrepancies. The border between ozone poor air inside the vortex and ozone rich air of midlatitudinal origin correspond with the vortex edge being defined with the help of the strongest horizontal mPV gradient. Unusual high ozone values measured inside the vortex are due to a measurement problem with the CRISTA instrument.

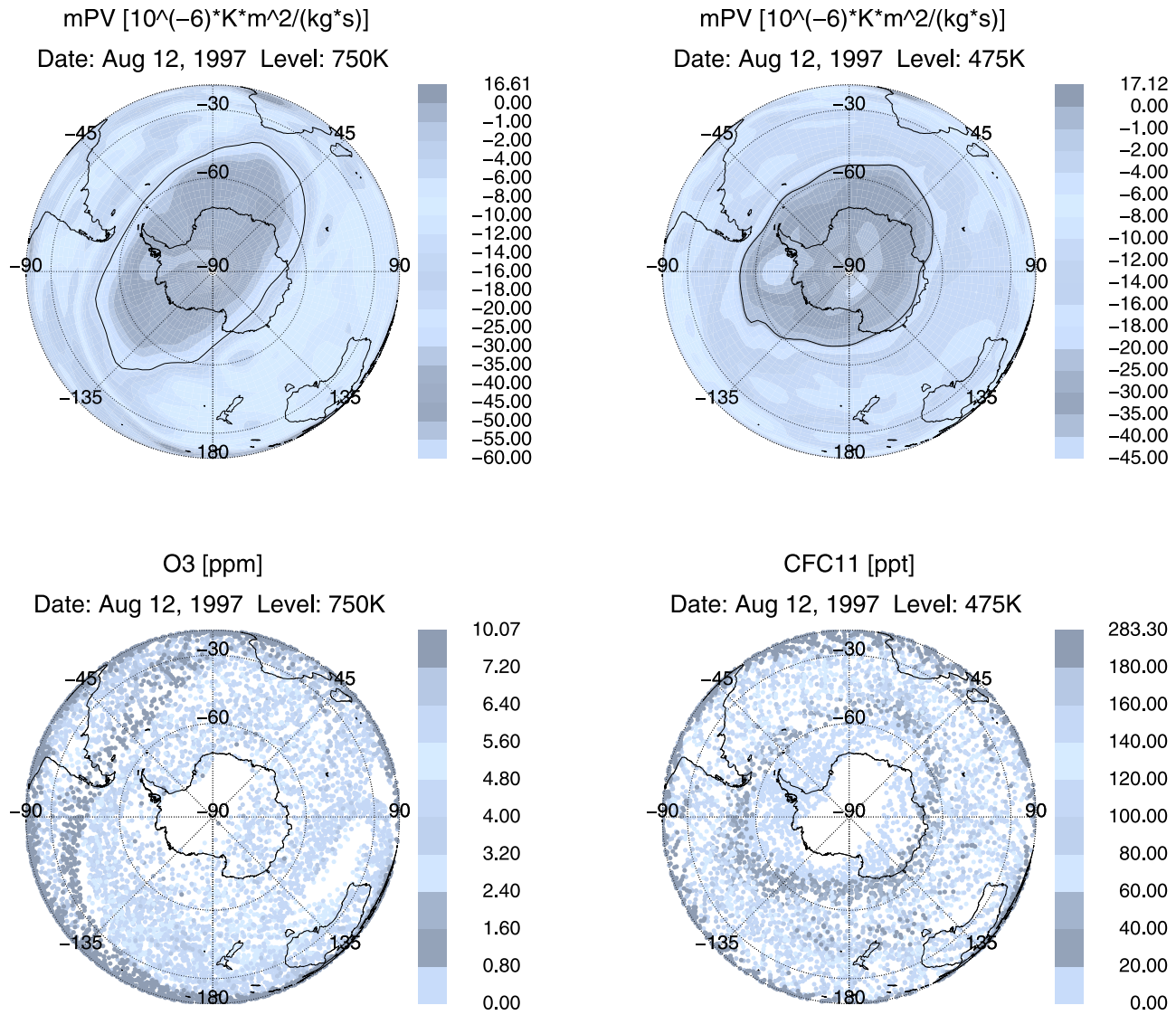

Figure 10. Modified PV on the 750 K (upper left) and the 475 K (upper right) isentropic surface on 12 August 1997. The thick black line denotes the vortex edge. Ozone (in ppm) on the 750 K (lower left) and CFC-11 (in ppt) on the 475 K isentropic level for 12 August measured by CRISTA 2. All measurements were made between 10 August (1200 UT) and 12 August (1200 UT) and mapped forward to 12 August (1200 UT) (see section 2). See color version of this figure at back of this issue.

[19] The streamer of subtropical air identified by high ozone values is clearly visible. The same holds true for the air masses with lower ozone values embedded into the anticyclone over South America, although there is a phase shift between the region of lower ozone and lower mPV. The second streamer of subtropical air moving along the vortex edge into the polar region between 45°E and 90°E is only discernible as a very small filament in the CRISTA data.

[20] The tongue of air masses being drawn from the vortex between 135°W and 175°W agree remarkably well with the mPV distribution. Air masses with ozone values typical for the vortex edge are observed in the region of the anticyclone south of Australia, resembling a much larger and consistent anticyclonic structure than the UKMO data. In general much more fine-scale structure can be observed in the CRISTA measurements. Strength and location of these features do not always coincide with the patterns in the mPV distribution.

[21] In the lower stratosphere the vortex showed a more asymmetric shape with two pronounced ridges and one weak ridge, rotating eastward as well (see Figure 10, upper right panel). The mPV gradient indicating the vortex edge is much smaller than in the middle stratosphere, thus allowing material more easily to be drawn from the vortex. The anticyclonic structures observed in the 750 K isentropic level (Figure 10, upper left panel) extended down to this height, but were shifted to the east due to a slight westward tilt with height (commonly observed with planetary waves). Again material was drawn from the polar vortex and transported equatorward in a small tongue heading toward New Zealand. The meridional exchange of air masses in general appears to be much smaller than in the middle stratosphere.

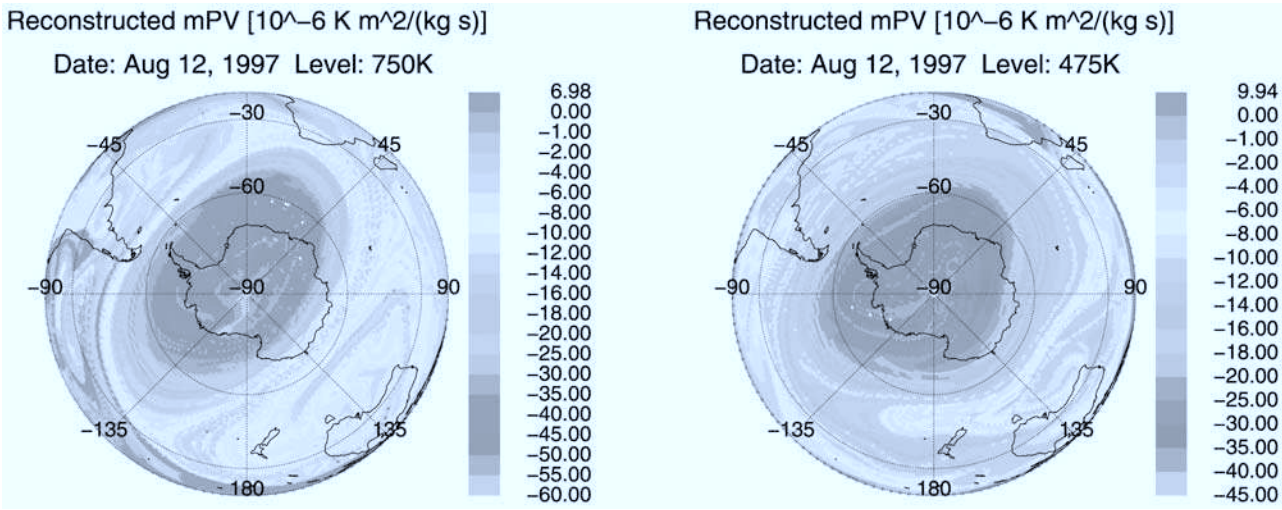

Figure 11. High-resolution reconstructed mPV fields from 10 day backward trajectory calculations for the 750 K (left) and 475 K (right) isentropic level for 12 August 1997. See color version of this figure at back of this issue.

[22] A comparison of the mPV distribution on the 475 K isentropic surface with CFC-11 observations made by CRISTA (Figure 10, lower right panel) again shows in general good agreement. With CFC-11 being a long lived tracer with tropospheric sources which enters the stratosphere mainly at the tropics, its distribution shows a strong meridional gradient which is enhanced by the subsidence of air inside the polar vortex. The area of low CFC-11 values matches the vortex area defined by the mPV criterion remarkably well. Due to the values of CFC-11 inside the vortex being near the detection limit of CRISTA no structures similar to those visible in Figure 10 (upper right panel) can be recognized. Air masses with CFC-11 values indicating that they originate in the vortex edge region could be observed forming a tongue like structure extending from the vortex edge to New Zealand and Australia. In the area of the anticyclone south of Australia a filament with high CFC-11 values can be observed representing air moving poleward from the tropics and being coiled up counterclockwise. Again these features are much more pronounced in the CRISTA data than in the mPV distribution.

3. RDF Simulations

[23] The modified PV fields and observations made by CRISTA showed air masses having been pulled off the polar vortex or drawn from subtropical regions and moved poleward thus indicating meridional transport of material. Some of the features could be recognized in both data sets, some were visible only in one data set and barely discernible in the other. This may be due to different reasons, the most important one being that the tracer distributions analyzed show different horizontal gradients, thus pronouncing different features depending on where they originate. Another problem is that some of the observed features are of too small a scale to be represented in a proper way by the mPV distribution based on data being on the coarse UKMO grid.

[24] To get a more detailed and complete picture of the flow pattern during this episode, reverse nonisentropic trajectory calculations [*Sutton et al.*, 1994] are used to generate simulated high-resolution mPV fields. This method has been used successfully for analyzing transport processes [see, e.g., *Fairlie et al.*, 1997; *Manney et al.*, 1998]. The trajectory model used is described by *Sutton et al.* [1994]. Cross-isentropic transport is taken into account by applying a diabatic correction term utilizing an improved version [*Zhong and Haigh*, 1995] of the Morcrette radiation scheme [*Morcrette*, 1991]. The trajectory model as a part of the CLaMS model system is described in more detail by *McKenna et al.* [2002].

[25] The results presented here are based on 10 day backward trajectories using UKMO winds. Each isentropic level is represented by about 30000 air parcels resulting in a horizontal grid resolution of about 90 km. During the calculation the air parcels show diabatic descent inside the polar vortex of between 1 and 2 K per day at the 475 K and 750 K isentropic level, respectively. This is in good agreement with the calculations done by *Rosenfield et al.* [1994] and *Sparling et al.* [1997].

[26] The quantity shown in the following is mPV calculated from reconstructed PV, hereafter referred to as reconstructed mPV. Figure 11 shows reconstructed mPV for 12 August on the 750 K (left panel) and 475 K (right panel) isentropic surfaces. The reconstructed mPV shows for both levels more small-scale structures than the mPV distributions derived from UKMO data (Figure 10, upper row). Because of the higher resolution the vortex edges are represented by a much sharper gradients. In addition, the vortex boundary region shows many filaments being peeled off both the inner and outer flank of the vortex edge. Although these can be observed in both levels, this process seems to be stronger in the lower stratosphere. The distribution of reconstructed mPV (Figure 11, right panel) shows the formation of filaments at the vortex boundary suggesting that air masses from this region are mixing into the vortex. Those filaments moving into the interior of the

vortex contribute to the structure of the inner vortex, which is very different from that suggested by the UKMO data. At the outer flank of the boundary region a filament can be observed wrapping almost once around the vortex. Although it seems that in some areas of the vortex and its boundary region the CFC-11 measurements made by CRISTA (Figure 10, lower right panel) support the results of the RDF simulations, in general no significant statement can be made about the inner vortex structure due to data gaps, measurement problems or the detection limits of the instrument.

[27] In the middle stratosphere (Figure 11, left panel) the air masses coming from the subtropics moving along the vortex edge are much better resolved and therefore more pronounced than in the UKMO data. Especially in the areas south of Australia and over South America where the filaments of low latitudinal origin coil up around the anticyclones the RDF results are more consistent with the CRISTA ozone measurements (Figure 10, lower left panel). The same hold true for the material being drawn from the vortex in a tongue like structure moving into the regions north of New Zealand.

[28] In the lower stratosphere the feature of a long streamer of air masses originating in the vortex edge being transported across New Zealand and toward Australia measured by CRISTA (Figure 10, lower right panel) is clearly visible. The filament of subtropical air wrapping around the anticyclonic structure south of Australia can be seen in the CRISTA data as well. While the UKMO data show almost no structure in the southern Atlantic region, both CRISTA data and the reconstructed mPV distribution indicate an exchange of air masses between the subtropics and the polar regions.

4. Summary

[29] The austral winter of 1997 was characterized by strong wave activity, with the main wave components being the eastward traveling zonal wave 1 and 2. The planetary waves were stronger than in most of the 15 preceding austral winters, resulting in heavy perturbation of the Antarctic polar vortex. The temperatures in the Antarctic polar regions were cold enough to allow for the formation of PSCs. On several occasions PSCs were detected by the CRISTA instrument.

[30] In August when the second CRISTA mission took place, the vortex in the middle stratosphere was forced into elliptical shape slowly rotating eastward about the pole. During that period the meteorological situation in the upper troposphere and lower stratosphere led to a pronounced local uplift of the tropopause resulting in an ozone minihole event.

[31] The edge of the middle stratospheric Antarctic vortex was characterized by a strong horizontal mPV gradient providing a barrier to cross boundary transport. In the lower stratosphere the boundary region became weaker, thus allowing air masses to be transported out of the vicinity of the edge into the interior of vortex. The exchange of material between the subtropical and the polar region took place mainly in form of small-scale features like streamers and narrow filaments. A comparison with CRISTA data shows that the resolution of the UKMO data is not high enough to resolve these flow patterns sufficiently, thus leading to apparent discrepancies between the measurements and the low-resolution PV fields.

[32] High-resolution mPV obtained by reverse nonisentropic trajectory calculations shows more atmospheric variability than is apparent in the UKMO data. The reconstructed mPV maps are more consistent with the measurements made by CRISTA, thus showing the advantages of RDF analyses of complex dynamical flow patterns with small-scale structures.

[33] **Acknowledgments.** The authors would like to thank the CRISTA group and the UK Met Office for providing the data. Thanks to the members of the CLaMS modeling group at Forschungszentrum Jülich for helpful discussions, and to Nicole Thomas and Reimar Bauer for programming support. The CRISTA 2 project was funded by the Bundesministerium für Bildung und Forschung through Deutsches Zentrum für Luft- und Raumfahrt (DLR) under contract 50 QV 9802-4.

References

Andrews, D. G., J. R. Holton, and C. B. Leovy, *Middle Atmosphere Dynamics*, Academic, San Diego, Calif., 1987.

Brinksma, E. J., et al., Analysis of record-low ozone values during the 1997 winter over Lauder, New Zealand, *Geophys. Res. Lett.*, *25*, 2785–2788, 1998.

Fairlie, T. D., R. B. Pierce, W. L. Grose, G. Lingenfelser, M. Loewenstein, and J. R. Podolske, Lagrangian forecasting during ASHOE/MAESA: Analysis of predictive skill for analyzed and reverse-domain-filled potential vorticity, *J. Geophys. Res.*, *102*, 13,169–13,182, 1997.

Grossmann, K. U., D. Offermann, O. Gusev, J. Oberheide, M. Riese, and R. Spang, The CRISTA 2 Mission, *J. Geophys. Res.*, *107*, doi:10.1029/2001JD000667, in press, 2002.

Hild, L., A. Richter, F. Wittrock, M. Weber, A. Ladstädter-Weißenmayer, R. Spang, K. U. Grossmann, and J. P. Burrows, A study of PSC activation of chlorine during the austral winter 1997, in *Proceedings for the European Symposium on Atmospheric Measurements From Space*, vol. 1, pp. 343–346, ESTEC, Nordwijk, Netherlands, 1999.

Hoerling, M. P., T. D. Schaack, and A. J. Lenzen, Global objective tropopause analysis, *Mon. Weather Rev.*, *119*, 1816–1831, 1991.

Lait, L. R., An alternative form for potential vorticity, *J. Atmos. Sci.*, *51*, 1754–1759, 1994.

Lehmacher, G., and D. Offermann, *CRISTA/MAHRSI Campaign 2 Handbook*, University of Wuppertal, 1997.

Manney, G. L., J. D. Farrara, and C. R. Mechoso, The behaviour of wave 2 in the southern hemisphere stratosphere during late winter and early spring, *J. Atmos. Sci.*, *48*, 976–998, 1991.

Manney, G. L., J. C. Bird, D. P. Donovan, T. J. Duck, J. A. Whiteway, S. R. Pal, and A. I. Carswell, Modeling ozone laminae in ground-based Arctic wintertime observations using trajectory calculations and satellite data, *J. Geophys. Res.*, *103*, 5797–5814, 1998.

McKenna, D. S., R. L. Jones, J. Austin, E. V. Browell, M. P. McCormick, A. J. Krueger, and A. F. Tuck, Diagnostic studies of the Antarctic vortex during the 1987 Airborne Antarctic Ozone Experiment: Ozone miniholes, *J. Geophys. Res.*, *94*, 11,641–11,668, 1989.

McKenna, D. S., P. Konopka, J.-U. Grooß, G. Günther, R. Müller, R. Spang, D. Offermann, and Y. Orsolini, A new Chemical Lagrangian Model of the Stratosphere (CLaMS), 1, Formulation of advection and mixing, *J. Geophys. Res.*, *107*(D16), 4309, doi:10.1029/2001JD000114, 2002.

Morcrette, J.-J., Radiation and cloud radiative properties in the European Centre for Medium-Range Weather Forecasts forecasting system, *J. Geophys. Res.*, *96*, 9121–9132, 1991.

Offermann, D., K.-U. Grossmann, P. Barthol, P. Knieling, M. Riese, and R. Trant, Cryogenic Infrared Spectrometers and Telescopes for the Atmosphere (CRISTA) experiment and middle atmosphere variability, *J. Geophys. Res.*, *104*, 16,311–16,325, 1999.

Peter, T., Microphysics and heterogeneous chemistry of polar stratospheric clouds, *Annu. Rev. Phys. Chem.*, *48*, 785–822, 1997.

Riese, M., G. L. Manney, J. Oberheide, X. Tie, and D. Offermann, Stratospheric transport by planetary wave mixing as observed during CRISTA 2, *J. Geophys. Res.*, *107*(D23), 8179, doi:10.1029/2001JD000629, 2002.

Rosenfield, J. E., P. A. Newman, and M. R. Schoeberl, Computations of diabatic descent in the stratospheric polar vortex, *J. Geophys. Res.*, *99*, 16,677–16,689, 1994.

Spang, R., M. Riese, and D. Offermann, CRISTA 2 observations of the south polar vortex in winter 1997: A new data set for polar process studies, *Geophys. Res. Lett.*, *28*, 3159–3162, 2001.

Sparling, L. C., J. A. Kettleborough, P. H. Haynes, M. E. McIntyre, J. E. Rosenfield, M. R. Schoeberl, and P. A. Newman, Diabatic cross-isentropic dispersion in the lower stratosphere, *J. Geophys. Res.*, *102*, 25,817–25,829, 1997.

Sutton, R. T., H. Maclean, R. Swinbank, A. O'Neill, and F. W. Taylor, High-resolution stratospheric tracer fields estimated from satellite observations using Lagrangian trajectory calculations, *J. Atmos. Sci.*, *51*, 2995–3005, 1994.

Swinbank, R., and A. O'Neill, A stratosphere-troposphere data assimilation system, *Mon. Weather Rev.*, *122*, 686–702, 1994.

Zhong, W., and J. D. Haigh, Improved broadband emissivity parameterization for water vapor cooling rate calculations, *J. Atmos. Sci.*, *52*, 124–138, 1995.

G. Günther, Forschungszentrum Jülich, Institute for Stratospheric Chemistry (ICG-1), D-52425 Jülich, Germany. (g.guenther@fz-juelich.de)

D. S. McKenna, Atmospheric Chemistry Division, National Center for Atmospheric Research, 1850 Table Mesa Drive, Boulder, CO 80307-3000, USA. (danny@acd.ucar.edu)

R. Spang, EOS Space Research Center, University of Leicester, University Road, Leicester, LE1 7RH, UK. (r.spang@le.ac.uk)

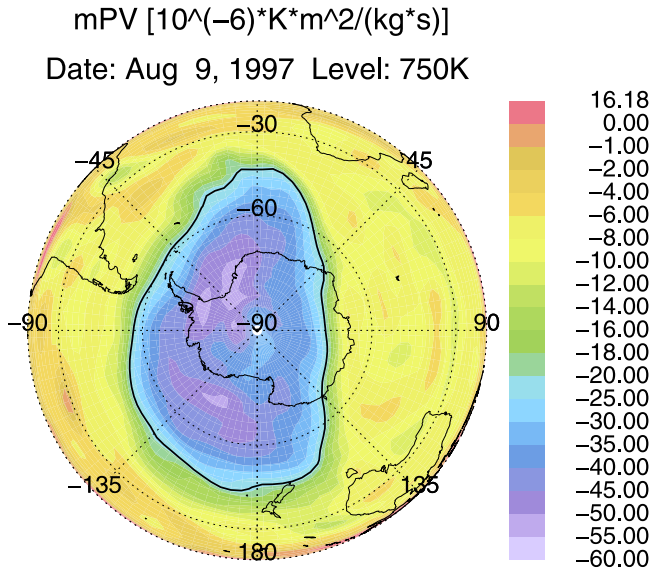

Figure 7. Modified PV on the 750 K isentropic surface on 9 August 1997. The thick black line denotes the vortex edge.

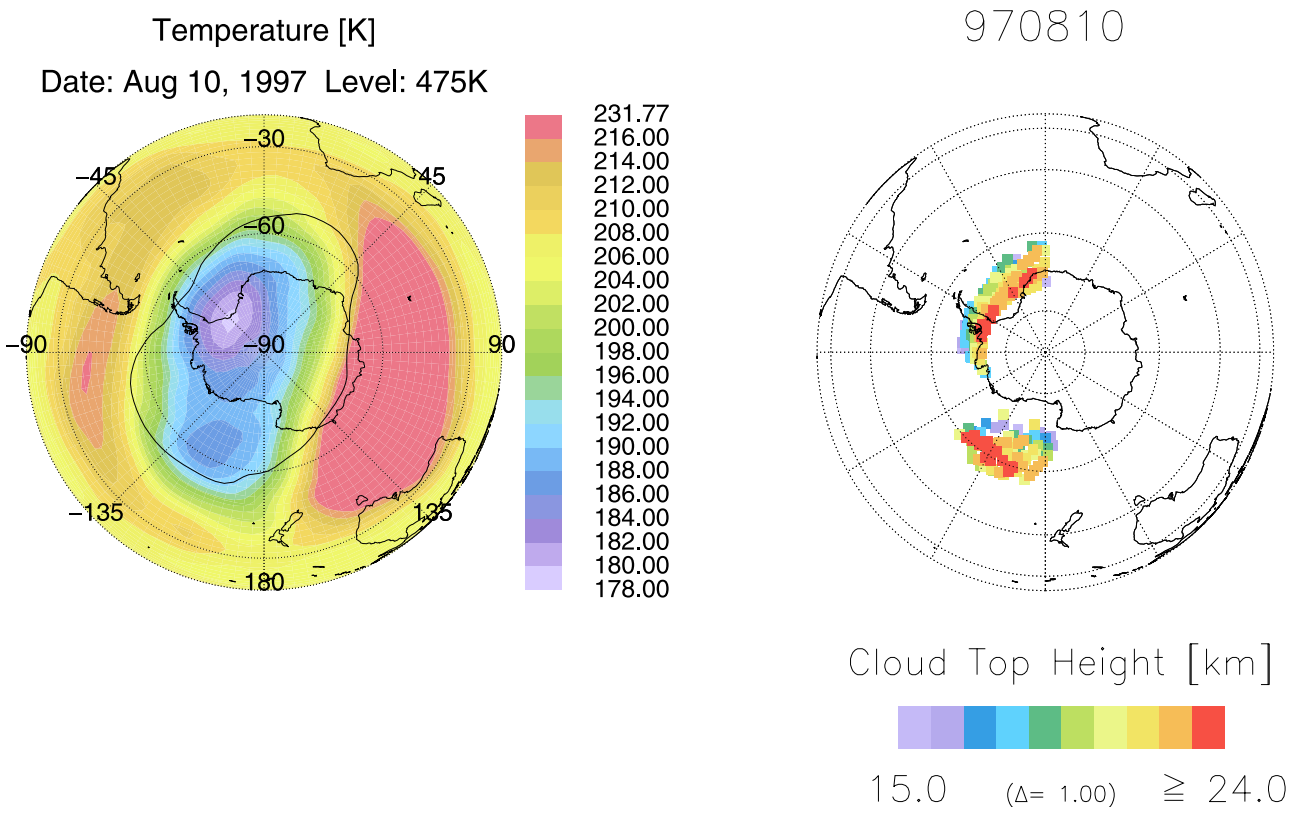

Figure 8. Temperature distribution on the 475 K isentropic level (left) and cloud top height calculated from CO_2 and aerosol measurements by CRISTA 2 (right) for 10 August. The thick black line in the left panel denotes the vortex edge.

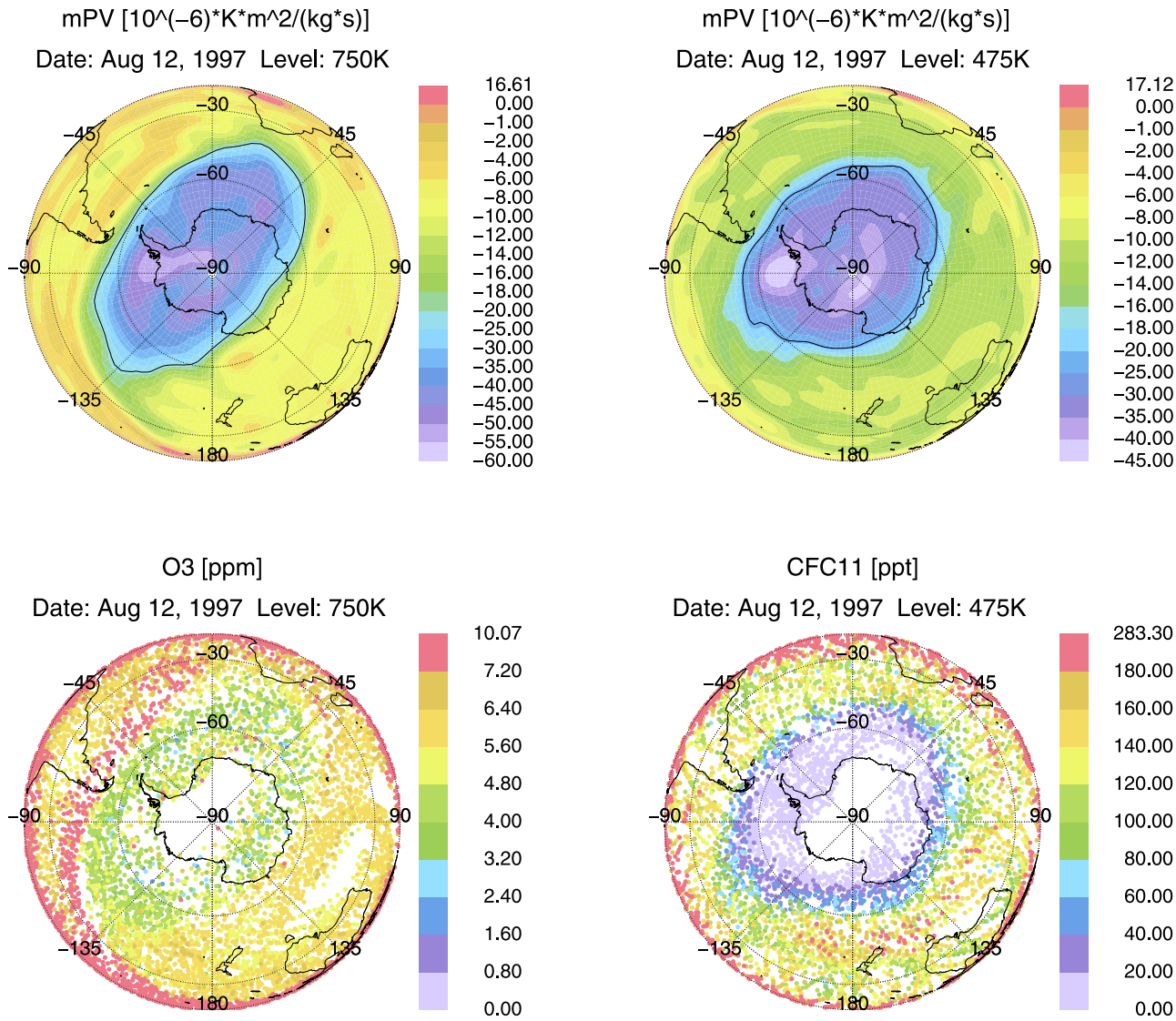

Figure 10. Modified PV on the 750 K (upper left) and the 475 K (upper right) isentropic surface on 12 August 1997. The thick black line denotes the vortex edge. Ozone (in ppm) on the 750 K (lower left) and CFC-11 (in ppt) on the 475 K isentropic level for 12 August measured by CRISTA 2. All measurements were made between 10 August (1200 UT) and 12 August (1200 UT) and mapped forward to 12 August (1200 UT) (see section 2).

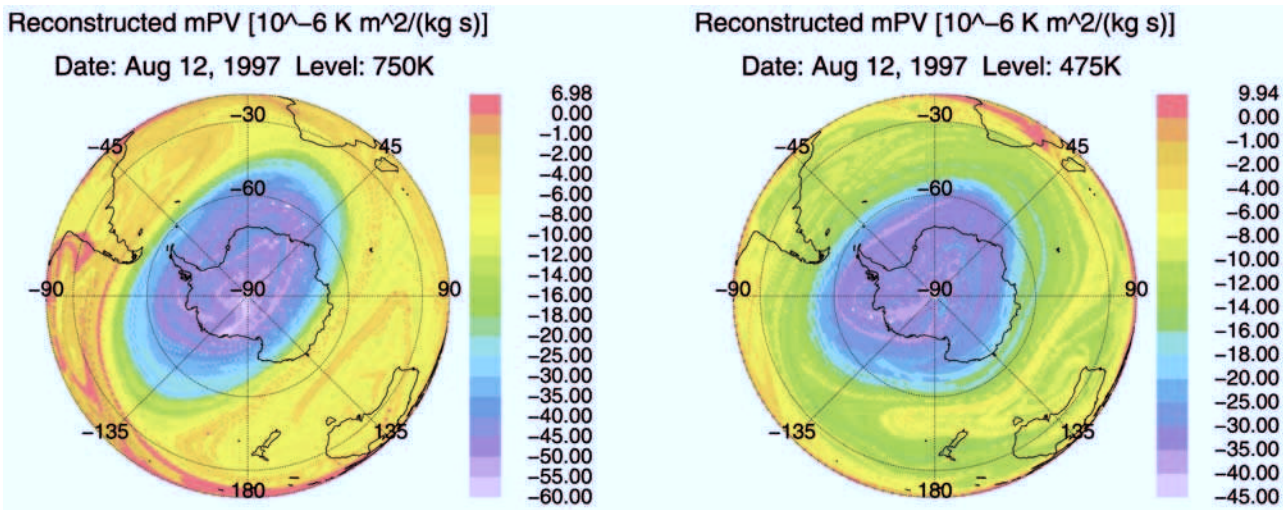

Figure 11. High-resolution reconstructed mPV fields from 10 day backward trajectory calculations for the 750 K (left) and 475 K (right) isentropic level for 12 August 1997.